



African dust particles over the western Caribbean – Part I: Impact on air quality over the Yucatán Peninsula

Carolina Ramírez-Romero¹, Alejandro Jaramillo¹, María F. Córdoba^{1,2}, Graciela B. Raga¹, Javier Miranda³, Harry Alvarez-Ospina⁴, Daniel Rosas⁵, Talib Amador⁵, Jong Sung Kim⁶, Jacqueline Yakobi-Hancock⁶, Darrel Baumgardner⁷, and Luis A. Ladino¹

¹Centro de Ciencias de la Atmósfera, Universidad Nacional Autónoma de México, Mexico City, Mexico

²Posgrado en Ciencias Químicas, Universidad Nacional Autónoma de México, Mexico City, Mexico

³Instituto de Física, Universidad Nacional Autónoma de México, Mexico City, Mexico

⁴Facultad de Ciencias, Universidad Nacional Autónoma de México, Mexico City, Mexico

⁵Facultad de Química, Universidad Autónoma de Yucatán, Mérida, Yucatán, Mexico

⁶Department of Community Health and Epidemiology, Dalhousie University, Halifax, Nova Scotia, Canada

⁷Droplet Measurement Technologies, Colorado, USA

Correspondence: Luis A. Ladino (luis.ladino@atmosfera.unam.mx)

Received: 19 April 2020 – Discussion started: 16 June 2020

Revised: 9 November 2020 – Accepted: 24 November 2020 – Published: 12 January 2021

Abstract. On a global scale, African dust is known to be one of the major sources of mineral dust particles, as these particles can be efficiently transported to different parts of the planet. Several studies have suggested that the Yucatán Peninsula could be influenced by such particles, especially in July, associated with the strengthening of the Caribbean low-level jet. Although these particles have the potential to significantly impact the local air quality, as shown elsewhere (especially with respect to particulate matter, PM), the arrival and impact of African dust in Mexican territory has not been quantitatively reported to date.

Two short-term field campaigns were conducted to confirm the arrival of African dust on the Yucatán Peninsula in July 2017 and July 2018 at the Mérida atmospheric observatory (20.98° N, 89.64° W). Aerosol particles were monitored at ground level using different online and off-line sensors. Several PM_{2.5} and PM₁₀ peaks were observed during both sampling periods, with a relative increase in the PM levels ranging between 200 % and 500 % with respect to the normal background conditions. Given that these peaks were found to be highly correlated with supermicron particles and chemical elements typically found in mineral dust particles, such as Al, Fe, Si, and K, they are linked with African dust. This conclusion is supported by combining back trajectories with vertical profiles from radiosondes, reanalysis, and satellite images to

show that the origin of the air masses arriving at Mérida was the Saharan Air Layer (SAL). The good agreement found between the measured PM₁₀ concentrations and the estimated dust mixing ratio content from MERRA-2 (Version 2 of the Modern-Era Retrospective analysis for Research and Applications) corroborates the conclusion that the degradation of the local (and likely regional) air quality in Mérida is a result of the arrival of African dust.

1 Introduction

The second largest natural contribution of atmospheric particles, worldwide, after sea spray, is mineral dust (Pey et al., 2013). Although volcanoes and soil dust from agricultural activities are significant sources of mineral dust (Walker, 1981; Tegen et al., 2004), the largest sources are the deserts that are distributed around the world (Goudie and Middleton, 2006). Africa is considered one of the most important of these sources as it emits ca. 800 Tg yr⁻¹, corresponding to ca. 70 % of the global dust (Prospero et al., 2014; Ryder et al., 2019). Therefore, African dust particles play a significant role in the climate system, as they can affect the planetary radiative balance and the hydrological cycle. Their optical properties, i.e., scattering and absorption, modulate radiative

forcing, and these particles also impact cloud formation and evolution as they can act as cloud condensation nuclei and/or ice-nucleating particles (Zhang et al., 2007; Hoose and Möhler, 2012; DeMott et al., 2015; Kanji et al. 2017). Additionally, several studies have shown that the presence of mineral dust can influence tropical cyclone formation (Dunion and Velden, 2004; Evan et al., 2006) and human health, as these particles degrade air quality (Carlson and Prospero, 1972; Prospero, 1999; Prospero et al., 2014; Venero-Fernández, 2016).

African dust particles are efficiently transported far from their emission source (Perry et al., 1997; Chiapello et al., 1997). According to Middleton and Goudie (2001), there are different trajectories that African dust experiences around the world. Among the most important, African dust particles can be transported to the western Mediterranean and Europe (Karanasiou et al., 2012; Perez et al., 2008; Prodi and Fea, 1979; Salvador et al., 2014), to the eastern Mediterranean and the Middle East (Ganor and Mamane, 1982; Ganor et al., 2010; Athanasopoulou et al., 2016), and towards the southern African continent (d'Almeida, 1986; Resch et al., 2008). Additionally, African dust is transported across the Atlantic Ocean to the United States, Mexico, the Caribbean region, and South America (Prospero et al. 1981; Bravo et al., 1982; Perry et al., 1997; Chiapello et al., 1997; Prospero and Lamb, 2003; Venero-Fernández, 2016; Barkley et al., 2019; Kramer et al., 2020). The long-range transport of African dust over the Atlantic represents 25 % of the total emissions from the Saharan Desert (Shao et al., 2011). This transport is favored in the Northern Hemisphere during the summer (i.e., from June to September) within a dry and hot elevated layer called the Saharan Air Layer (SAL) (Carlson and Prospero, 1972; Prospero and Carlson, 1972; Karyampudi and Carlson, 1988; Tsamalis et al., 2013; Weinzierl et al., 2016).

During the summer, the SAL ascends to altitudes between 5 and 7 km through interactions with cool marine air masses (Adams et al., 2012; Chouza et al., 2016; Korte et al., 2018). Dunion and Velden (2004), Dunion and Marron (2008), and Dunion (2011) studied the characteristics of the air masses that reach the North Atlantic and the Caribbean region during the boreal summer months. They found that there are three distinct air masses: a moist tropical air mass (MT), the SAL, and midlatitude dry air intrusions (MLDAIs). Each type of air mass is associated with unique thermodynamic and kinematic characteristics, and they have a wide range of possible origins. However, the SAL and MLDAI air masses have distinct flow patterns across the North Atlantic, which allows one to differentiate between these masses by tracking their origin. In contrast, their distinctly unique moisture characteristics allow for the differentiation of the MT from SAL air masses (Dunion, 2011).

There are different methods for the detection of the long-range transport of African dust and its presence in different regions around the world. For several decades, the tracking of dust events has been studied using remote sensing (Chiapello

et al., 1999; Dunion and Velden, 2004; Foltz and McPhaden, 2008; Prospero et al., 2002; Liu et al., 2008; Voss and Evan, 2020). Ground- and space-based tools such as light detection and ranging (LIDAR) and satellite sensors (e.g., the Moderate Resolution Imaging Spectroradiometer, MODIS, and the Visible Infrared Imaging Radiometer Suite, VIIRS) provide the aerosol spatial distribution with altitude in terms of the aerosol optical depth (AOD), mass concentration, and particle size distribution (Zhang and Reid, 2006; Jackson et al., 2013).

Another useful tool is the reanalysis from global climate models that assimilates, in a statistically optimal way, satellite and ground observations. The reanalysis produces continuous, four-dimensional fields of different atmospheric variables of interest, contrasting with the observations that may be spatially and temporally sparse (Cohn, 1997; Kalnay, 2003; Rienecker et al., 2011; Schutgens et al., 2010). The use of reanalysis, considering its inherent uncertainties, has become an essential tool in the atmospheric research community (Gelaro et al., 2017). For example, the Hybrid Single-Particle Lagrangian Integrated Trajectory (HYSPLIT) model has been successfully used to track the transport of African dust particles (e.g., Ashrafi et al., 2014; Prospero et al., 2005). HYSPLIT uses meteorological data from different modeling sources, including the NCEP–NCAR (National Centers for Environmental Prediction–National Center for Atmospheric Research) reanalysis model (Stein et al., 2015).

The transport of African dust can also be evaluated with the NASA Global Modeling and Assimilation Office (GMAO) MERRA-2 reanalysis (Prospero et al., 2020). MERRA-2 (Version 2 of the Modern-Era Retrospective analysis for Research and Applications) is the first multidecadal reanalysis that assimilates both meteorological and aerosol data from various ground- and space-based remote sensing sources (Gelaro et al., 2017; Randles et al., 2017). Despite some deficiencies, previous studies have demonstrated that the MERRA-2 aerosol assimilation system does indeed show considerable skill in simulating numerous observable aerosol properties (e.g., Buchard et al., 2015, 2016, 2017; Randles et al., 2017). MERRA-2 has been previously used to study the effects of aerosol particles in the Earth system in several studies focused on dust-related phenomena. For example, Buchard et al. (2017) showed the benefit of the MERRA-2 assimilation for the retrieval of the seasonality, vertical distribution, and magnitude of the dust surface concentrations during an episode of dust transport from Africa to the Caribbean. Later on, Veselovskii et al. (2018) showed the consistency of the MERRA-2 aerosol products with Mie–Raman lidar observations performed in West Africa during a smoke and dust mixing event. Similarly, Grogan and Thornicrof (2019) studied the characteristics of African easterly waves and their relationship with synoptic-scale plumes of Saharan mineral dust. More recently, Bibi et al. (2020) studied atmospheric dust load and deposition fluxes along the North African coast

of the Mediterranean Sea, and Aldhaif et al. (2020) studied dust events impacting the East Coast of the United States.

The in situ monitoring of aerosol properties, such as aerosol size and mass distribution, is very useful to determine their influence on local air quality and human health (Querol et al., 2019). Hence, different studies have been carried out in the Caribbean islands and Florida to quantify the impact of African dust on the local air quality (Prospero, 1999; Prospero and Mayol-Bracero, 2013; Prospero et al., 2014). In Barbados, the monitoring of the atmospheric aerosol mass began in 1965, whereas in Miami, Florida, it began in 1974 and continues to the present (Prospero and Mayol-Bracero, 2013). In Barbados, it is estimated that 50 % of the $PM_{2.5}$ (i.e., particulate matter with an aerodynamic diameter $D < 2.5 \mu\text{m}$) and ca. 90 % of the PM_{10} (i.e., $D < 10 \mu\text{m}$) consist of African dust (Li-Jones and Prospero, 1998; Prospero et al., 2001; Reid et al., 2003a). In Miami, the mean daily mass concentration of mineral dust during the summer typically ranges between 10 and $100 \mu\text{g m}^{-3}$, with a large interannual variability (Prospero et al., 2001). During the Puerto Rico Dust Experiment (PRIDE) campaign, the mineral dust concentration at the ground level was found to exceed $70 \mu\text{g m}^{-3}$ (Reid et al., 2003b). In the aforementioned studies, the African dust particles transported over the Atlantic affected the local air quality, exceeding the World Health Organization (WHO) guidelines for $PM_{2.5}$ and PM_{10} . According to WHO, air pollution and its effects are considered a global health priority (WHO, 2002). Several studies have linked high concentrations of mineral dust (in terms of $PM_{2.5}$ and PM_{10}) to brain, skin, lung, cardiovascular, cerebrovascular, and respiratory diseases (Alessandrini et al., 2013; Goudie, 2014; Wilker et al., 2015; Brook et al., 2010; Dominici et al., 2006; Zhang et al., 2016). Additionally, African dust particles have been found to serve as carriers for biological material. Griffin et al. (2001) reported the presence of viable bacteria and fungi associated with the arrival of African dust over the Virgin Islands (United States). Similarly, Rodriguez-Gomez et al. (2020) found a higher concentration of viable bacteria and fungal propagules during summer than during winter on the Yucatán Peninsula, with summer being the season when African dust intrusions are more frequent.

The chemical and mineralogical composition of particles also plays an important role in the identification of African dust in the receptor regions (Nenes et al., 2014). The most abundant minerals present in these particles are silicates (quartz), clay minerals (kaolinite, illite, chlorite, palygorskite), feldspars (albite, anorthite), and carbonates (calcite) (Goudie and Middleton, 2006; Querol et al., 2019; Broadley et al., 2012). The major oxides in Saharan dust are SiO_2 , Al_2O_3 , Fe_2O_3 , CaO , MgO , and K_2O , as well as (to a lesser extent) P_2O_5 and TiO_2 (Goudie and Middleton, 2006; Linke et al., 2006). Several studies in the Caribbean have identified high levels of Fe and Al in dust events (Prospero et al., 2001; Rosinski et al., 1988). Additionally, Rosinski et

al. (1988) reported high percentages of Si and Mg in particles collected in the Gulf of Mexico (GoM) during July.

Although the arrival of African dust in Mexico has been suggested for decades (e.g., Bravo et al., 1982; Prospero, 1999; Lenes et al., 2012), to our knowledge, there has not been a comprehensive study, published in the open, peer-reviewed literature, that documents this atmospheric phenomenon. For the first time, in this study we document the arrival of African dust on the Yucatán Peninsula for two consecutive years (i.e., 2017 and 2018) using in situ and remote sensing measurements, reanalysis, back trajectory analysis, and complementary meteorological observations.

2 Materials and methods

2.1 Sampling site and field campaigns

The Yucatán Peninsula is located in the southeast of Mexico. It borders the GoM to the north; the Atlantic Ocean to the east; and the Caribbean Sea, Guatemala, and Belize to the south. The Yucatán has characteristics that are unique to this region (Plasencia, 1998). For example, its uniform terrain, the absence of rivers, and the type of soil, which is formed by Cretaceous sediments that do not present mineralization and are rich in calcium, commonly called “Laja de Yucatán” (Plasencia, 1998) sets the Yucatán aside from other regions of Mexico. The average temperature of the Yucatán Peninsula ranges from 25 to 35 °C (World Resource Institute, 2018) with an average annual relative humidity of 79 % (INEGI, 2009). The Peninsula has a warm, semidry climate on the coast and a warm, subhumid climate throughout the rest of the region, with a rainy season between summer and autumn (June–October) (Orellana et al., 2009; ProAire, 2018). Precipitation in this region is mainly due to convective activity, and it is influenced by the moisture advection by the trade winds (Orellana et al., 2009; ProAire, 2018). In situ measurements were made in the city of Mérida, situated in the northeast sector of the Yucatán Peninsula (20.98° N, 89.64° W), which is the capital of the Yucatán state. Mérida has 892 363 inhabitants (INEGI, 2015) and is 23 km from the coast. The most representative activities in the region are tourism, commerce, and the textile industry (INEGI, 2017).

Aerosol particles were continuously monitored with sensors installed at the School of Chemistry of the Universidad Autónoma de Yucatán (FC-UADY), located in the central-western part of the city (Fig. 1), as part of the African Dust And Biomass Burning Over Yucatan (ADABBOY) project. Table 1 lists the instrumentation used to characterize particle physical, optical, and chemical properties. The Partisol and MiniVol were installed on the rooftop of the FC-UADY, whereas the other instruments were maintained in an environmentally controlled area where they sampled from inlets connected to a ventilated chimney that extended approximately 1.5 m above the roof. This measurement site is

Table 1. Summary of the measured variables and the instrumentation used.

Measured variable	Instrumentation
Particle mass concentration	PM _{2.5} and PM ₁₀ analyzer (FH 62 C14, Thermo Fisher Scientific Inc.)
Total particle concentration ($d > 50$ nm)	Condensation particle counter (CPC, 3010, TSI)
Particle size distribution ($d > 300$ nm)	Optical particle counter (Lasair II 310A, MSP)
Aerosol collection (PM ₁₀ and PM _{2.5})	Partisol (2525, Thermo Fisher Scientific Inc.) and MiniVol (3380, Airmetrics)
Nitrogen oxides (NO _x); Ozone (O ₃)	NO _x analyzer (Model 42i, Thermo Fisher Scientific Inc.); O ₃ analyzer (Model 49i, Thermo Fisher Scientific Inc.)
Temperature and relative humidity; precipitation; wind direction and wind speed; solar radiation	<i>T</i> and HR sensor (VAISALA, HMP115); pluviometer (Texas Electronics, TR-525M); wind direction and wind speed sensor (Gill, 1405-PK-100); radiation pyrometer (Intertek, 20W)
Absorption coefficient; particle-bound polycyclic aromatic hydrocarbon (pPAH) concentration	Soot absorption photometer PSAP (Radiance Research); photoacoustic spectroscopy (PAS 2000, Ecochem)

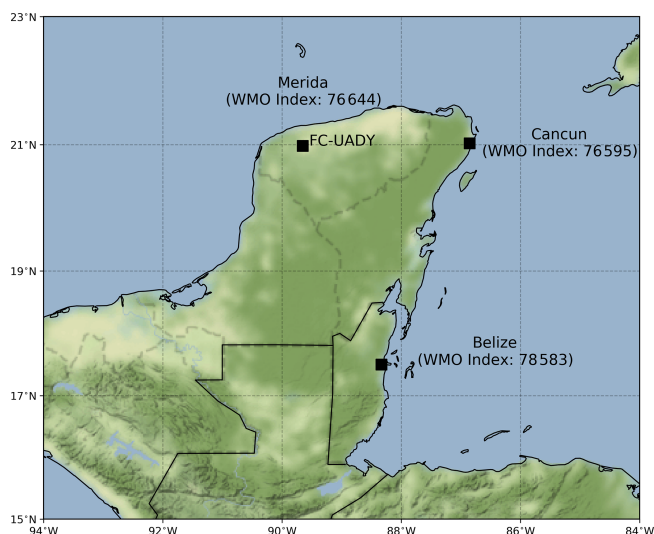


Figure 1. Location of the sampling site at the School of Chemistry of the Autonomous University of Yucatán (FC-UADY) and the three World Meteorological Organization (WMO) radiosonde stations located on the Yucatán Peninsula: Mérida International Airport, Mexico (WMO index: 76 644); Cancún, Mexico (WMO index: 76 595); and Philip S. W. Goldson International Airport, Belize (WMO index: 78 583).

part of the University Network of Atmospheric Observatories (RUOA) supported by the National University of Mexico (UNAM). Two intensive sampling periods were conducted between 11–31 July 2017 and 30 June–17 July 2018.

2.2 Aerosol concentration and particle size distribution

The particulate mass concentration was monitored continuously with PM_{2.5} and PM₁₀ analyzers providing real-time measurements (FH 62 C14, Thermo Fisher Scientific Inc.) with a temporal resolution of 1 min at a sampling flow rate of 16.7 L min⁻¹ (Thermo Fisher Scientific Inc., 2007).

The total number concentration of particles with sizes approximately larger than 50 nm was measured by a condensation particle counter (CPC 3010, TSI) at a sampling rate of 1 Hz with a flow rate of 1.0 L min⁻¹, and the aerosol number concentration as a function of particle size was monitored by an optical particle counter (Lasair II 310A, MSP). The Lasair has six different size bins (0.3, 0.5, 1.0, 5.0, 10.0, and 25 μm), a flow rate of 28.3 L min⁻¹, and a time resolution of 11 s.

2.3 Aerosol collection and chemical composition analysis

PM_{2.5} and PM₁₀ aerosol particles were collected for 24 h with a Partisol model 2525 (Thermo Fisher Scientific Inc.) and for 48 h with a Minivol (3380, Airmetrics) on 47 mm Teflon filters (Pall Science). The MiniVol and Partisol flow rates were 5.0 and 16.7 L min⁻¹, respectively. After the sampling periods, the filters were placed in 60 mm Petri dishes and stored at 4 °C prior to the chemical analysis.

Elemental analysis was performed on each filter using X-ray fluorescence (XRF) with the X-ray spectrometer at Laboratorio de Aerosoles, Instituto de Física, UNAM (Espinosa et al., 2012). The X-ray tube was made by Oxford Instruments (Scotts Valley, CA, USA), and a Rh anode and an Amptek X-123 SDD spectrometer (Bedford, MA, USA) were used. The samples were irradiated for 900 s working with a current

of 500 μA and resulting in a spectrum that was analyzed using the WinQXAS computer code (IAEA, 1997). The product of this analysis derived mass concentrations of Fe, Al, Si, Ca, Na, P, Mg, Mn, Ti, Cl, P, Zn, K, S, Cu, and Ni along with their associated uncertainties, as described by Espinosa et al. (2010).

2.4 Meteorological and satellite data

The local and regional meteorological conditions were monitored using different approaches. The RUOA meteorological sensors were placed at the rooftop of the FC-UADY (Table 1) and continuously measured the wind speed and direction, air temperature, relative humidity, solar radiation, and precipitation. To derive the regional and vertical distribution of meteorological conditions, radiosondes and reanalysis were used. The information provided by the radiosondes launched was from three World Meteorological Organization (WMO) stations on the Yucatán Peninsula, as shown in Fig. 1, located at Mérida (Mérida International Airport, Mexico (WMO index: 76 644), Cancún (WMO index: 76 595), and Belize (Philip S.W. Goldson International Airport, Belize; WMO index: 78 583). The processed radiosonde data were obtained from the University of Wyoming (<http://weather.uwyo.edu/upperair/sounding.html>, last access: 20 March 2020).

Hourly total precipitable water vapor and three-dimensional 3-hourly aerosol mixing ratio data were obtained from the MERRA-2 reanalysis (GMAO, 2015a, b). The aerosol properties in MERRA-2 were simulated with the Goddard Chemistry Aerosol Radiation and Transport model (GOCART), which takes the sources, sinks, and chemistry of 15 externally mixed aerosol mass mixing ratio tracers into account: dust (five noninteracting size bins), sea salt (five noninteracting size bins), hydrophobic and hydrophilic black and organic carbon (BC and OC, respectively; four tracers), and sulfate (SO_4) (Randles et al., 2017; Buchard et al., 2017).

The air mass back trajectories were calculated using the HYSPLIT model from the National Oceanic and Atmospheric Administration (NOAA). In conjunction with the in situ measurements, the back trajectories were calculated considering the maximum concentration of PM reported by the $\text{PM}_{2.5}$ and PM_{10} analyzers. The trajectories were initiated at 250 and 500 m a.g.l. going backward in time for 13 d. Although Kramer et al. (2020) reported that mineral dust particles arrive in Miami ca. 10 d after they are produced in North Africa, they may take longer to reach the Yucatán Peninsula. The different heights of the HYSPLIT back-trajectory runs were chosen to determine the rate of descent of dust air masses to the surface. Also considered was the AOD measured with the MODIS instruments on the Aqua and Terra satellites.

3 Results and discussion

3.1 Local evidence

Several studies have shown that air quality ($\text{PM}_{2.5}$ and PM_{10}) significantly deteriorates upon the arrival of African dust plumes (Prospero and Lamb, 2003; Prospero et al., 2001, 2014; Prospero and Mayol-Bracero, 2013). Figure 2 shows the time series of the $\text{PM}_{2.5}$ and PM_{10} concentrations for the July–August periods of 2017 and 2018. Some high-concentration PM peaks are clearly identified, with $\text{PM}_{2.5}$ and PM_{10} values as high as 54 and 135 $\mu\text{g m}^{-3}$, respectively. Henceforth these peaks will be referred to in our study as African dust peaks (ADPs). Note that the background concentration (defined as the lowest values within the sampling period where the chemical composition was available) of $\text{PM}_{2.5}$ is $\sim 4 \mu\text{g m}^{-3}$, and the background concentration of PM_{10} is $\sim 10 \mu\text{g m}^{-3}$. The ADPs found in 2017 (i.e., 22–24 July, 27–28 July, and 4, 6–7 August) resulted in an increase of 300 % in $\text{PM}_{2.5}$ and 500 % in PM_{10} with respect to background conditions. In 2018, the ADPs (i.e., 10–11 July, 13–15 July, 16–17 July, 23–26 July, and 9–10 August) exceeded 200 % and 300 % of the background levels of $\text{PM}_{2.5}$ and PM_{10} , respectively. The aforementioned ADPs not only exceeded the $\text{PM}_{2.5}$ and PM_{10} thresholds suggested by WHO (i.e., $\text{PM}_{2.5} = 25 \mu\text{g m}^{-3}$ and $\text{PM}_{10} = 50 \mu\text{g m}^{-3}$, 24 h mean) but more than double them, as was the case for the 9–12 August 2018 event. Similar behavior has been previously observed in Puerto Rico, Miami, and Barbados upon the arrival of African dust particles (Reid et al., 2003b; Prospero et al., 2005, 2014). The mass concentrations of $\text{PM}_{2.5}$ and PM_{10} were found to be 49 % and 54 % higher in 2018 than in 2017, respectively, suggesting a higher frequency or intensity of African dust plumes arriving over Mérida in 2018.

Figure 2 also shows the elemental composition obtained from the XRF analysis (16 elements) for five ADPs observed during the 2017 and 2018 field campaigns. In addition, 1 d from each field campaign was selected to determine the elemental background composition. The selected days are 10–11 July in 2017 and 6 July in 2018. These days were chosen because the $\text{PM}_{2.5}$ and PM_{10} concentrations were within the mean background values and did not include any atypical peak nor apparent external influence.

High levels of sodium (Na, pink), chlorine (Cl, turquoise blue), sulfur (S, dark orange), and calcium (Ca, light green) were found in the background samples, corresponding to > 70 % of the total mass (Fig. 2). The presence of Na and Cl are expected in airborne particles at this site given the city's proximity to the GoM (i.e., 23 km away). Cerón et al. (2002) reported large concentrations of Na, Cl, and Mg that originated from sea salt, when analyzing the composition of rainwater from the Yucatán Peninsula. The high levels of S can be associated with local anthropogenic activities such as vehicular, ship, and industrial emissions (e.g., Corbett and Fischbeck, 1997; Cerón-Bretón et al., 2018). Additionally, given

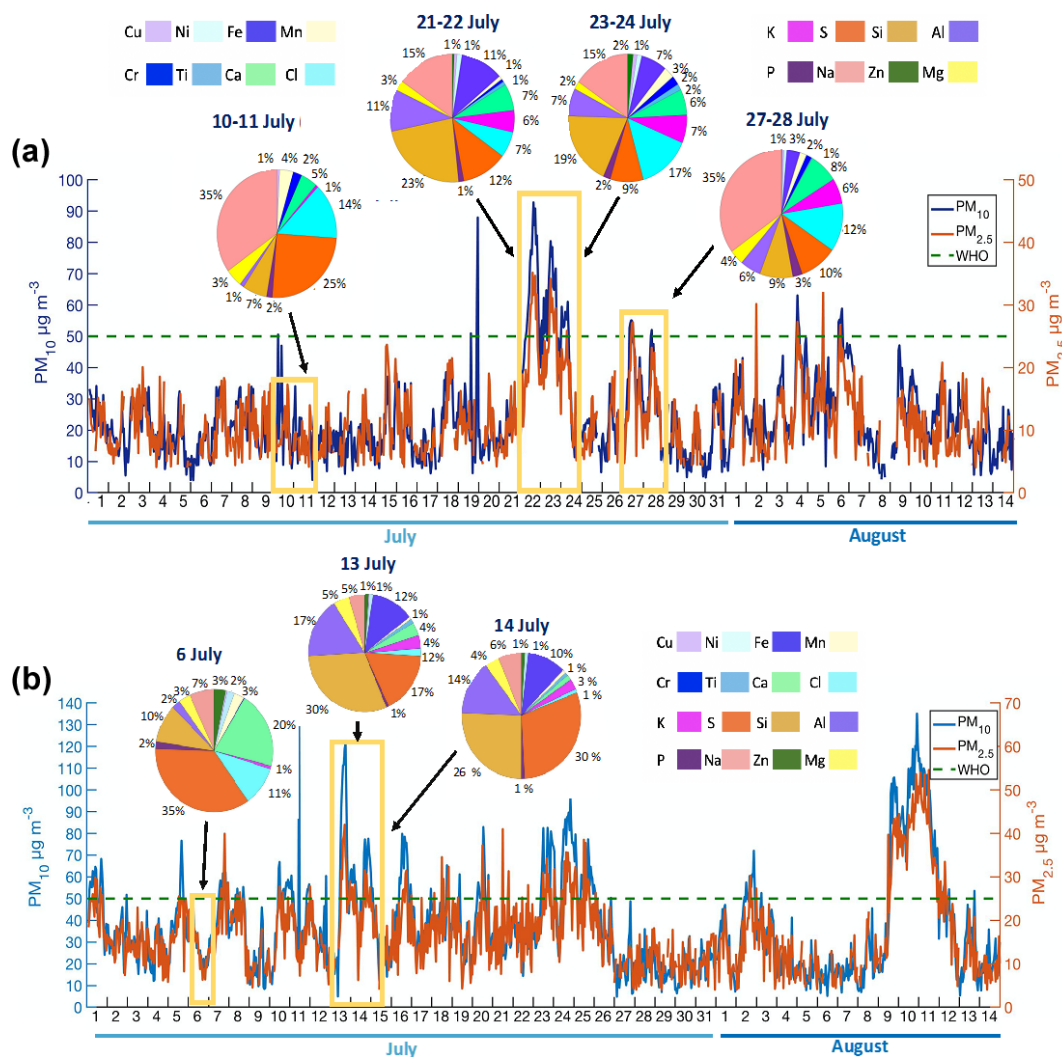


Figure 2. Mass concentrations of $\text{PM}_{2.5}$ and PM_{10} in (a) 2017 and (b) in 2018. The green horizontal line depicts the World Health Organization air quality guideline for 24 h mean $\text{PM}_{2.5}$ (right y axis) and PM_{10} (left y axis) concentrations of 25 and $50 \mu\text{g m}^{-3}$, respectively (WHO, 2002). The pie charts represent the elemental composition from the XRF for the African dust peaks (ADPs).

the short distance between Mérida and the GoM, it is possible that dimethylsulfide (DMS) production from plankton in the GoM could be a natural source of S, as has been shown in other studies (e.g., Rosinski et al., 1988; Kloster et al., 2006; Vallina and Simó, 2007). Finally, the presence of Ca could be related to the limestone soil prevalent on the Yucatán Peninsula and the resuspension of road dust (Plasencia, 1998; Querol et al., 2019).

Interestingly, the elemental composition of the airborne particles collected during the ADPs showed higher concentrations of silica (Si, dark yellow), aluminum (Al, light purple), and iron (Fe, dark purple) than those in the background particles (Fig. 2). While the Si concentrations are approximately 3 times larger than the baseline, Al and Fe increased by 8 and 12 times, respectively. To corroborate the relationship between the increase in PM and the African dust, each

of the 16 elements analyzed by XRF were correlated with the $\text{PM}_{2.5}$ and PM_{10} concentrations. Of the 16 elements Al, Si, K, and Fe were the only ones with correlation coefficients $r > 0.6$ ($p < 0.05$) for both years, as shown in Fig. S1. The present results are in agreement with previous studies that showed high correlation coefficients between the aforementioned elements (e.g., Caquineau et al., 1998; Guieu et al., 2002; Trapp et al., 2010). Also, the concentration of aerosol particles with diameters between 0.5 and $25 \mu\text{m}$, as measured by the Lasair, were found to be highly correlated with the $\text{PM}_{2.5}$ and PM_{10} concentrations, $r = 0.79$ and $r = 0.87$, respectively (Fig. S2). Finally, the typical background particle size distribution showed significant changes during the arrival of ADPs for particles ranging between 0.5 and $5.0 \mu\text{m}$ (Fig. S3). It is widely known that the typical size of African dust particles transported over long distances ranges from 0.1

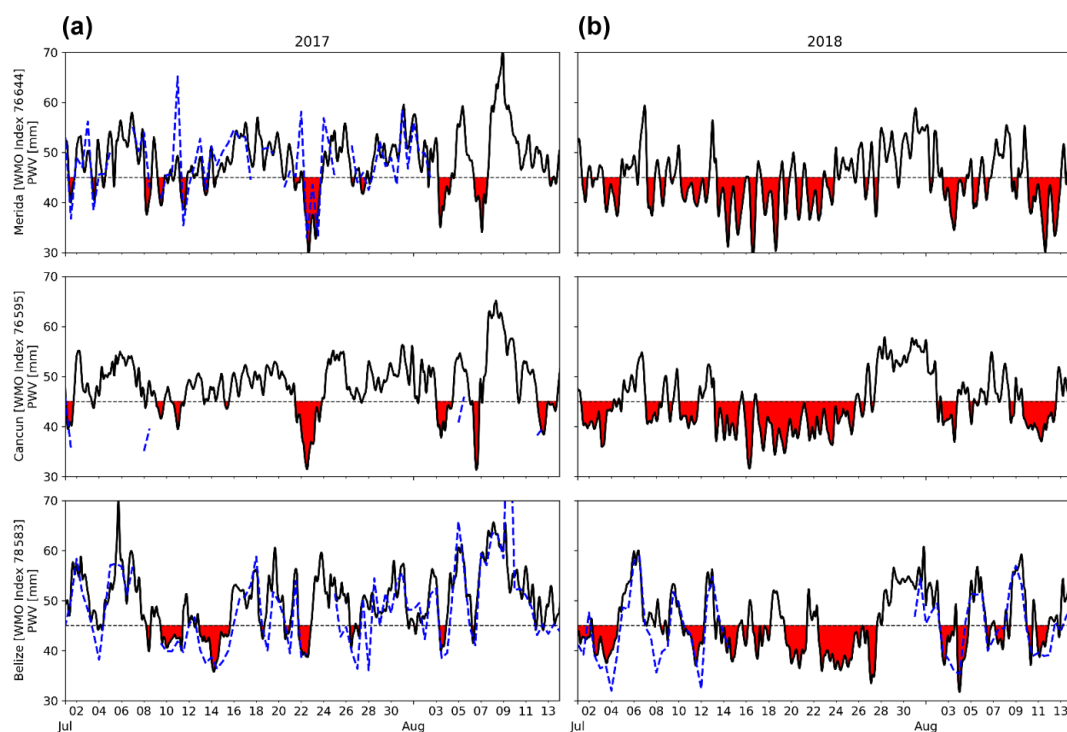


Figure 3. MERRA-2 precipitable water (black solid line) and precipitable water values estimated from radiosonde measurements (blue dashed line), for the three WMO radiosonde stations located on the Yucatán Peninsula for (a) July–August 2017 and (b) July–August 2018. The red areas represent the periods where precipitable water vapor (PWV) is less than 45 mm.

to 20 μm (e.g., Bégue et al., 2012; Denjean et al. 2016). Overall, the high concentration of coarse particles and the increase in Al, Si, and Fe during the ADPs, together with the good correlations found between the $\text{PM}_{2.5}$ and PM_{10} concentrations with Al, Si, K, Fe, and particles larger than 0.5 μm strongly suggests that the ADPs are mineral particles associated with dust transported from Africa to Mexico.

Additionally, it is important to note that Al, Si, K, and Fe are common oxides found in African dust composed of minerals and clays such as quartz (SiO_2), kaolinite ($\text{Al}_2\text{Si}_2\text{O}_5(\text{OH})_4$), illite ($(\text{K},\text{H}_3\text{O})(\text{Al},\text{Mg},\text{Fe})_2(\text{Si},\text{Al})_4\text{O}_{10}[(\text{OH})_2,(\text{H}_2\text{O})]$), chlorite ($((\text{Mg},\text{Fe})_5\text{Al})(\text{AlSi}_3\text{O}_{10}(\text{OH})_8)$), palygorskite ($(\text{Mg},\text{Al})_2\text{Si}_4\text{O}_{10}(\text{OH}) \cdot 4(\text{H}_2\text{O})$), and feldspars such as albite ($\text{NaAlSi}_3\text{O}_8$), anorthite ($\text{CaAl}_2\text{Si}_2\text{O}_8$), and orthoclase (KAlSi_3O_8), among others (Goudie and Middleton, 2006; Linke et al., 2006; Broadley et al., 2012; Querol et al., 2019). Rosinski et al. (1988) reported that up to 90 % of the collected airborne particles in the presence of dust events in the GoM contained Al, Fe, and Si. In Puerto Rico, Reid et al. (2003b) found that the concentrations of Si and Al on aerosol particles ($> 0.74 \mu\text{m}$) were above 10 and 5 $\mu\text{g m}^{-3}$, respectively, during dust events that reached the island. Similarly, Prospero et al. (2001) reported concentrations of Al $> 1.0 \mu\text{g m}^{-3}$ and Fe $> 0.5 \mu\text{g m}^{-3}$ on $\text{PM}_{2.5}$ on days

when high concentrations of African dust particles were reported in Miami.

To confirm that no aerosol sources other than the African dust were the origin of the high PM peaks observed in Mérida in July 2017 and 2018, the $\text{PM}_{2.5}$ and PM_{10} concentrations were correlated with other measured variables. As shown in Figs. S2 and S4, $\text{PM}_{2.5}$ and PM_{10} concentrations are poorly correlated ($r < 0.09$) with local pollution emissions such as particle-bound polycyclic aromatic hydrocarbons (pPAHs), black carbon (inferred from the absorption coefficient), and nitrogen oxides (NO_x). Note that those gases and particles can be considered as proxies of anthropogenic pollutants generated by the incomplete combustion of fossil fuels and biomass burning, as previously demonstrated for Mérida (Muñoz-Salazar et al., 2020; Alvarez-Ospina et al., 2020). Also, correlation coefficients below 0.29 were found between O_3 and solar radiation with the $\text{PM}_{2.5}$ and PM_{10} concentrations indicating that it is very unlikely that secondary organic particles could be the source of the ADPs observed in Mérida, as was the case in high particle concentration events shown by Muñoz-Salazar et al. (2020).

Finally, although none of the different meteorological variables monitored at the surface level were found to correlate with the $\text{PM}_{2.5}$ and PM_{10} concentrations, as shown by the wind roses in Fig. S5, easterly winds were prevalent when

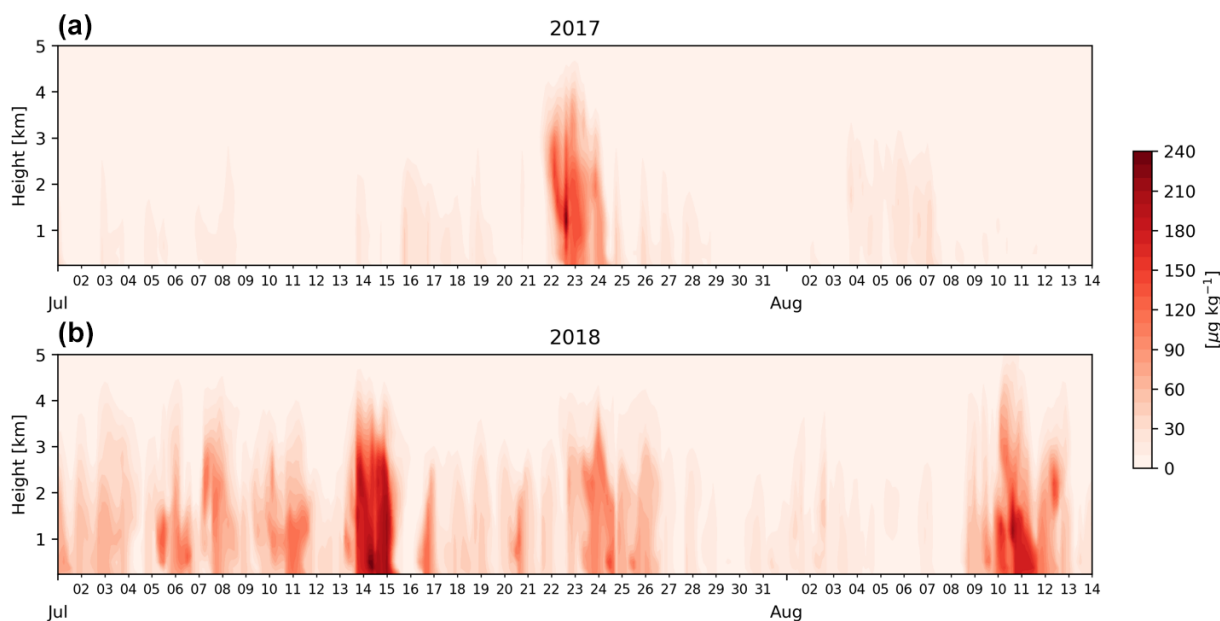


Figure 4. The 3 h time series of the vertical profile of the estimated dust content from MERRA-2 for the 1 July–14 August period for (a) 2017 and (b) 2018 for the Mérida region.

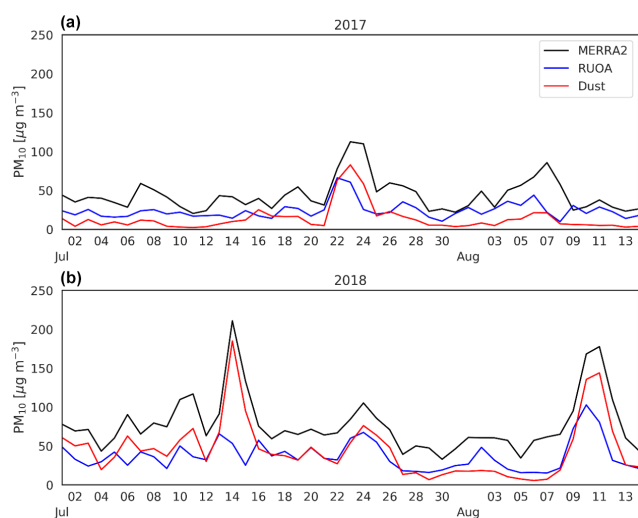


Figure 5. Daily mean of PM_{10} estimated from MERRA-2 (black line), PM_{10} measured by the RUOA station (blue line), and the estimated dust mixing ratio content from MERRA-2 (red line) for (a) 2017 and (b) 2018.

ADPs were observed. This is relevant as African dust can only be transported by easterly winds.

3.2 Larger-scale observations

To evaluate the source of the ADPs observed in Mérida from a large-scale perspective, we focus on the classification of tropical air masses in the North Atlantic and the Caribbean region during the boreal summer months proposed

by Dunion (2011). We used HYSPLIT to estimate the trajectories of different air masses that reached Mérida during the July–August periods of 2017 and 2018. HYSPLIT trajectories for the 2017 and 2018 ADPs point to an African origin and, therefore, suggest that these air masses are either MT or SAL (See Fig. S6). To differentiate the MT from SAL, we focused on their distinctly unique moisture characteristics. Dunion (2011) proposes that a threshold of 45 mm of total precipitable water vapor (PWV), which corresponds to the total amount of water vapor contained in the atmospheric column from the surface to the top of the troposphere (AMS, 2000), can be used to differentiate dry from moist air masses. This value is consistent with other studies that use PWV to identify dry-air days (e.g., Hanks and Marinaro, 2016), and as deep tropical convection begins to increase above a critical PWV value of 50 mm (Holloway and Neelin, 2009). Note that PWV is given by the vertical integral of the mixing ratio $x(p)$ at the pressure level p in the layer bounded by pressures p_1 and p_2 and can be calculated using Eq. (1) (AMS, 2000):

$$\text{PWV} = \frac{1}{\rho g} \int_{p_1}^{p_2} x dp, \quad (1)$$

where ρ represents the density of water, and g is the acceleration of gravity.

Figure 3 shows the time series of PWV for the July–August 2017 and 2018 periods at each WMO radiosonde site. The black solid line shows PWV from MERRA-2, available from the Vertically Integrated Diagnostics (GMAO, 2015a), together with PWV estimated using Eq. (1) from the available radiosonde profiles shown as the dashed blue lines. One

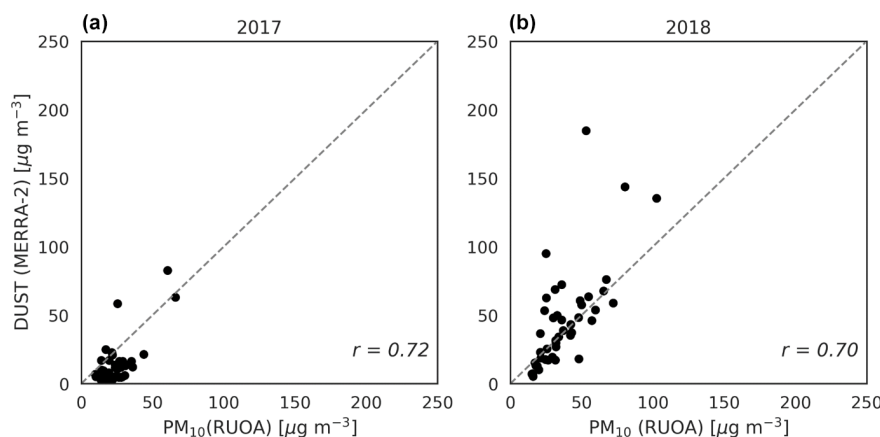


Figure 6. Dispersion diagrams of the surface dust mixing ratio from MERRA-2 (y axis) vs. the PM_{10} from the RUOA station for the periods shown in Fig. 5 for (a) 2017 and (b) 2018.

caveat is that there is a striking lack of radiosonde data in the periods of interest. Nevertheless, we can see good agreement between the available observed PWV and that of PWV from MERRA-2. Therefore, the latter can be used as a good approximation for PWV in the region to differentiate moist from dry air masses. In Fig. 3, the periods where PWV is less than 45 mm are highlighted in red. These periods show dry air masses that coincide with air mass trajectories with an African origin (i.e., 22–24 July, 27–28 July, and 4 and 6–7 August in 2017, and 10–12 July, 13–15 July, 16–17 July, 23–26 July, and 9–12 August in 2018), allowing us to conclude that these dry air masses have mainly SAL characteristics.

The arrival of African dust in Mérida was also explored from the MERRA-2 dataset. Figure 4 shows the time series of the estimated vertical profiles of the 3 h time series of the dust mixing ratio from MERRA-2 at Mérida for 2017 and 2018. It shows that the events corresponding to the arrival of dry air masses from Africa displayed in Fig. 3 nicely correlate with high dust mixing ratios, strongly supporting the hypothesis of SAL air reaching the Yucatán Peninsula. Figure 4 also shows that the July–August period of 2018 was particularly active with frequent arrivals of dust in the region, which is in agreement with the higher $\text{PM}_{2.5}$ and PM_{10} concentrations measured in 2018, as depicted in Fig. 2. Figure S7 focuses on the vertical profiles of the dust mixing ratio for the periods of 21–25 July 2017 and 12–16 July 2018. These periods show the increase in dust in the atmospheric column in the studied region, supporting the hypothesis that the source of the ADPs shown in Fig. 2 is likely African dust.

Finally, the arrival of African dust plumes over the Yucatán Peninsula was confirmed by investigating the AOD detected by the MODIS Aqua and Terra satellites for July 2017 and 2018, as shown in Figs. S8 and S9. Although this information cannot be used to perform quantitative analysis, the AOD images allow us to confirm the arrival of African dust plumes on the Yucatán Peninsula. Additionally, as in

Figs. 2, 3, and 4, the AOD images also show that the African dust plumes activity was higher in 2018 than in 2017. Previous studies have also used the AOD from MODIS to identify the arrival of African dust. For example, Koren et al. (2006) tracked the long-range transport of dust from the Bodélé Depression (north central Africa) to the Amazon Basin. Similarly, Kalashnikova and Kahn (2008) demonstrated that it is possible to observe the evolution of African dust plumes over the Atlantic Ocean with MODIS. Additionally, Kaufman et al. (2005) identified and quantified the transport and deposition of mineral dust over the Atlantic Ocean using MODIS data.

3.3 Comparison of in situ observations and reanalysis

The daily mean PM_{10} from MERRA-2 was estimated using the method proposed by Provençal et al. (2017). The black line in Fig. 5 shows the estimated PM_{10} , which is compared to the PM_{10} measured by the RUOA station in Mérida (blue line). The estimated surface dust mixing ratio from MERRA-2 is also shown in red. Figure 5 shows that MERRA-2 overestimates PM_{10} compared with ground-based measurements. Nevertheless, it should be clarified that the reanalysis information corresponds to a $0.5^\circ \times 0.625^\circ$ region, implying that MERRA-2 is estimating the regional average, whereas the station corresponds to a local measurement.

Despite these differences, Fig. 5 shows that the observations at the RUOA station have variations similar to those of MERRA-2. Figure 6 shows the dispersion diagram of the daily mean surface dust mixing ratio from MERRA-2 vs. PM_{10} measured from RUOA station for the periods indicated in Fig. 5. It shows a good correlation between the estimated dust and the measured PM_{10} – in particular for the 2018 period, which was especially active with constant arrivals of African dust to the region, as shown in Fig. 4. A similar analysis was performed for the 3 h estimated and

measured PM_{10} , as shown in Figs. S10 and S11, with identical conclusions to those for 24 h averages.

4 Conclusions

For the first time, the arrival of African dust into Mexican territory is quantitatively verified. The arrival of African dust particles in Mérida significantly degraded the local air quality as $PM_{2.5}$ and PM_{10} concentrations increased up to 500 % with respect to background conditions. Therefore, the presence of African dust in Mérida and the Yucatán Peninsula could be a potential health threat to their inhabitants. Although the African dust intrusions caused an increase in particulate matter in Mérida (Mexico), this increase is lower than those reported in other places closer to the Sahara, such as Barbados and the Mediterranean. In addition to the impacts on air quality, African dust particles can also be a serious health threat as they serve as a carrier of biological material originating in Africa, as reported by Rodríguez-Gomez et al. (2020). If the foreign biological particles are opportunistic pathogens, they can cause a variety of diseases in the receptor regions, such as the Yucatán Peninsula. Finally, these particles can impact the development of precipitation and affect the regional hydrological cycle when they serve as efficient ice-nucleating particles (e.g., Rosinski et al., 1988; Córdoba et al., 2020).

As shown in the present study, combining ground-based off-line and online sensors provides robust evidence of the arrival of African dust; however, we also show that the combination of back trajectories with radiosondes as well as the estimated surface dust mixing ratio from MERRA-2 are powerful tools that can be exploited when in situ information is missing, especially in developing countries where the necessary instrumentation is scarce.

Continuous monitoring of the arrival of African dust is of high importance not only in the Caribbean islands but also at other sites in Latin America such as Mexico, Belize, Guatemala, and Honduras. Additionally, epidemiological and statistical studies to track down the number of hospital admissions caused by respiratory issues before and after the arrival of African dust is urgently needed on the Yucatán Peninsula. This will allow policy-makers and local authorities to understand how strong the African dust impact is on local health and the need for better forecasting of such events.

Data availability. Data are available upon request from the corresponding author.

Supplement. The supplement related to this article is available online at: <https://doi.org/10.5194/acp-21-239-2021-supplement>.

Author contributions. CRR, GBR, and LAL designed the field campaigns and the experiments. CRR, MFC, HAO, DR, TA, and LAL carried out the aerosol measurements. CRR and AJ analyzed the remote sensing data. JM and HAO performed the chemical analyses. GBR, DB, DR, JSK, JYH, and LAL installed the equipment and provided the infrastructure for the ADABBOY project. CRR, AJ, and LAL wrote the paper, with contributions from all coauthors.

Competing interests. The authors declare that they have no conflict of interest.

Acknowledgements. The authors thank the University Network of Atmospheric Observatories (RUOA) for providing meteorological and criteria pollution data. Alejandro Jaramillo acknowledges the fellowship from DGAPA at UNAM. The authors also wish to express their gratitude to Elizabeth Garcia, Juan Carlos Pineda, Aline Cruz, and Javier Juarez for their invaluable help and support.

Financial support. This research has been supported by the Consejo Nacional de Ciencia y Tecnología (Conacyt; grant no. FC-2164) and the Universidad Autónoma de Yucatán (grant no. SISPROY-FQUI-2018-0003).

Review statement. This paper was edited by Sachin S. Gunthe and reviewed by Cassandra Gaston and two anonymous referees.

References

- Adams, A. A., Prospero, J. M., and Zhang, C.: CALIPSO – Derived Three-Dimensional Structure of Aerosol over the Atlantic Basin and Adjacent Continents, *J. Climate*, 25, 6862–6879, <https://doi.org/10.1175/JCLI-D-11-00672.1>, 2012.
- Aldhaif, A. M., Lopez, D. H., Dadashazar, H., and Sorooshian, A.: Sources, frequency, and chemical nature of dust events impacting the United States East Coast, *Atmos. Environ.*, 231, 117456 <https://doi.org/10.1016/j.atmosenv.2020.117456>, 2020.
- Alessandrini, E. R., Stafoggia, M., Faustini, A., Gobbi, G. P., and Forastiere, F.: Saharan dust and the association between particulate matter and daily hospitalizations in Rome, Italy, *J. Occup. Environ. Med.*, 70, 432–434, <https://doi.org/10.1136/oemed-2012-101182>, 2013.
- Alvarez-Ospina, H., Giordano, S., Ladino, L. A., Raga, G. B., Muñoz-Salazar, J., Leyte-Lugo, M., Rosas D., and Carabali G. Particle-bound polycyclic aromatic hydrocarbons (pPAHs) in Mérida, Mexico, *Aerosol Air Qual. Res.*, <https://doi.org/10.4209/aaqr.200245>, in press, 2020.
- AMS: Glossary of Meteorology, edited by: Glickman, T. S., American Meteorological Society, available at: <https://books.google.com.mx/books?id=kyhSAQAIAAJ>, ISBN 978-1-8782-2034-9, 2000.
- Ashrafi, K., Shafiepour-Motlagh, M., Aslemand, A., and Ghader, S.: Dust storm simulation over Iran using HYSPLIT, *J. Environ.*

- Health Sci. Eng., 12, 1–9, <https://doi.org/10.1186/2052-336X-12-9>, 2014.
- Athanasopoulou, E., Protonotariou, A., Papangelis, G., Tombrou, M., Mihalopoulos, N., and Gerasopoulos, E.: Long-range transport of Saharan dust and chemical transformations over the Eastern Mediterranean, *Atmos. Environ.*, 140, 592–604, <https://doi.org/10.1016/j.atmosenv.2016.06.041>, 2016.
- Barkley, A. E., Prospero, J. M., Mahowald, N., Hamilton, D. S., Pependorf, K. J., Oehlert, A. M., Pourmand, A., Gatineau, A., Panechou-Pulcherie, K., Blackwelder, P., and Gaston, C. J.: African biomass burning is a substantial source of phosphorus deposition to the Amazon, Tropical Atlantic Ocean, and Southern Ocean, *P. Natl. Acad. Sci. USA*, 116, 16216–16221, <https://doi.org/10.1073/pnas.1906091116>, 2019.
- Bibi, M., Saad, M., Masmoudi, M., Laurent, B., and Alfaro, S. C.: Long-term (1980–2018) spatial and temporal variability of the atmospheric dust load and deposition fluxes along the North-African coast of the Mediterranean Sea, *Atmos. Res.*, 234, 104689, <https://doi.org/10.1016/j.atmosres.2019.104689>, 2020.
- Bègue, N., Tulet, P., Chaboureau, J.-P., Roberts, G., Gomes, L., and Mallet, M.: Long-range transport of Saharan dust over north-western Europe during EUCAARI 2008 campaign: Evolution of dust optical properties by scavenging, *J. Geophys. Res.*, 117, D17201, <https://doi.org/10.1029/2012JD017611>, 2012.
- Bravo, J. L., Salazar, S., and Muhlia, A.: Mineral and sea salt aerosol concentrations over low latitude tropical Atlantic and Pacific oceans during FGGE, *Geo. Int.*, 20, 303–317, 1982.
- Broadley, S. L., Murray, B. J., Herbert, R. J., Atkinson, J. D., Dobbie, S., Malkin, T. L., Condliffe, E., and Neve, L.: Immersion mode heterogeneous ice nucleation by an illite rich powder representative of atmospheric mineral dust, *Atmos. Chem. Phys.*, 12, 287–307, <https://doi.org/10.5194/acp-12-287-2012>, 2012.
- Brook, R. D., Rajagopalan, S., Pope, C. A., Brook, J. R., Bhatnagar, A., Diez-Roux, A. V., Holguin, F., Hong, Y., Luepker, R. V., Mittleman, M. A., Peters, A., Siscovick, D., Smith, S. C., Whitsel, L., Kaufman, J. D., American Heart Association Council on Epidemiology and Prevention, Council on the Kidney in Cardiovascular Disease, and Council on Nutrition, Physical Activity and Metabolism: Particulate matter air pollution and cardiovascular disease: An update to the scientific statement from the American Heart Association, *Circulation*, 121, 2331–2378, <https://doi.org/10.1161/CIR.0b013e3181d8e1>, 2010.
- Buchard, V., da Silva, A. M., Colarco, P. R., Darmenov, A., Randles, C. A., Govindaraju, R., Torres, O., Campbell, J., and Spurr, R.: Using the OMI aerosol index and absorption aerosol optical depth to evaluate the NASA MERRA Aerosol Reanalysis, *Atmos. Chem. Phys.*, 15, 5743–5760, <https://doi.org/10.5194/acp-15-5743-2015>, 2015.
- Buchard, V., da Silva, A. M., Randles, C. A., Colarco, P., Ferrare, R., Hair, J., Hostetler, C., Tackett, J., and Winker, D.: Evaluation of the surface PM_{2.5} in Version 1 of the NASA MERRA Aerosol Reanalysis over the United States, *Atmos. Environ.*, 125, 100–111, <https://doi.org/10.1016/j.atmosenv.2015.11.004>, 2016.
- Buchard, V., Randles, C. A., Silva, A. M. da, Darmenov, A., Colarco, P. R., Govindaraju, R., Ferrare, R., Hair, J., Beyersdorf, A. J., Ziemba, L. D., and Yu, H.: The MERRA-2 Aerosol Reanalysis, 1980 Onward. Part II: Evaluation and Case Studies, *J. Climate*, 30, 6851–6872, <https://doi.org/10.1175/jcli-d-16-0613.1>, 2017.
- Caquineau, S., Gaudichet, A., Gomes, L., Magonthier, M. C., and Chatenet, B.: Saharan dust: Clay ratio as a relevant tracer to assess the origin of soil-derived aerosols, *Geophys. Res. Lett.*, 25, 983–986, <https://doi.org/10.1029/98GL00569>, 1998.
- Carlson, T. N., and Prospero, J. M.: The Large-Scale Movement of Saharan Air Outbreaks over the Northern Equatorial Atlantic, *J. Appl. Meteorol.*, 11, 283–297, [https://doi.org/10.1175/1520-0450\(1972\)011<0283:TLSMOS>2.0.CO;2](https://doi.org/10.1175/1520-0450(1972)011<0283:TLSMOS>2.0.CO;2), 1972.
- Cerón, R. M. B., Padilla, H. G., Belmont, R. D., Torres, M. C. B., Garcá, R. M., and Báez, A. P.: Rainwater chemical composition at the end of the mid-summer drought in the Caribbean shore of the Yucatan Peninsula, *Atmos. Environ.*, 36, 2367–2374, [https://doi.org/10.1016/S1352-2310\(02\)00169-3](https://doi.org/10.1016/S1352-2310(02)00169-3), 2002.
- Cerón-Bretón, R., Cerón-Bretón, J., Muriel-García, M., Lara-Severino, R., Rangel-Marrón, M., Ramírez-Lara, E., López-Jiménez, D., Rodríguez-Guzmán, A., and Uc-Chi, M.: Mapping of the atmospheric deposition of sulfur and nitrogen during the dry season 2016 in the Metropolitan zone of Merida, Yucatan, Mexico, *AIP. Conf. Proc.*, 182, 020021, <https://doi.org/10.1063/1.5045427>, 2018.
- Chiapello, I., Bergametti, G., Chatenet, B., Bousquet, P., Dulac, F., and Soares, E.S.: Origins of African dust transported over the northeastern tropical Atlantic, *J. Geophys. Res.*, 102, 13701–13709, <https://doi.org/10.1029/97JD00259>, 1997.
- Chiapello, I., Prospero, J. M., Herman, J. R., and Hsu, N. C.: Detection of mineral dust over the North Atlantic Ocean and Africa with the Nimbus 7 TOMS, *J. Geophys. Res.-Atmos.*, 104, 9277–9291, <https://doi.org/10.1029/1998JD200083>, 1999.
- Chouza, F., Reitebuch, O., Benedetti, A., and Weinzierl, B.: Saharan dust long-range transport across the Atlantic studied by an airborne Doppler wind lidar and the MACC model, *Atmos. Chem. Phys.*, 16, 11581–11600, <https://doi.org/10.5194/acp-16-11581-2016>, 2016.
- Cohn, S. E.: An Introduction to Estimation Theory (gtSpecial Issue: Data Assimilation in Meteorology and Oceanography: Theory and Practice), *J. Meteorol. Soc. Jpn. Ser. II*, 75, 257–288, https://doi.org/10.2151/jmsj1965.75.1B_257, 1997.
- Corbett, J. J. and Fischbeck, P.: Emissions from Ships, *Science*, 278, 823–824, <https://doi.org/10.1126/science.278.5339.823>, 1997.
- Córdoba, F., Ramírez-Romero, C., Cabrera, D., Raga, G. B., Miranda, J., Alvarez-Ospina, H., Rosas, D., Figueroa, B., Kim, J. S., Yakobi-Hancock, J., Amador, T., Gutierrez, W., Garcia, M., Bertram, A. K., Baumgardner, D., and Ladino, L. A.: Measurement report: Ice nucleating abilities of biomass burning, African dust, and sea spray aerosol particles over the Yucatan Peninsula, *Atmos. Chem. Phys. Discuss.*, <https://doi.org/10.5194/acp-2020-783>, in review, 2020.
- d’Almeida, G. A.: A Model for Saharan Dust Transport, *J. Climate Appl. Meteor.*, 25, 903–916, [https://doi.org/10.1175/1520-0450\(1986\)025<0903:AMFSDT>2.0.CO;2](https://doi.org/10.1175/1520-0450(1986)025<0903:AMFSDT>2.0.CO;2), 1986.
- DeMott, P. J., Prenni, A. J., McMeeking, G. R., Sullivan, R. C., Petters, M. D., Tobo, Y., Niemand, M., Möhler, O., Snider, J. R., Wang, Z., and Kreidenweis, S. M.: Integrating laboratory and field data to quantify the immersion freezing ice nucleation activity of mineral dust particles, *Atmos. Chem. Phys.*, 15, 393–409, <https://doi.org/10.5194/acp-15-393-2015>, 2015.
- Denjean, C., Formenti, P., Desboeufs, K., Chevaillier, S., Triquet, S., Maille, M., Cazaunau, M., Laurent, B., Mayol-Bracero, O. L., Vallejo, P., Quiñones, M., Gutierrez-Molina I. E., Cas-

- sola, F., Prati, P., Andrews, E., and Ogren, J.: Size distribution and optical properties of African mineral dust after intercontinental transport, *J. Geophys. Res.-Atmos.*, 121, 7117–7138, <https://doi.org/10.1002/2016JD024783>, 2016.
- Dominici, F., Peng, R. D., Bell, M. L., Pham, L., McDermott, A., Zeger, S. L., and Samet, J. M.: Fine particulate air pollution and hospital admission for cardiovascular and respiratory diseases, *JAMA*, 295, 1127–1134, <https://doi.org/10.1001/jama.295.10.1127>, 2006.
- Dunion, J. P.: Rewriting the climatology of the tropical North Atlantic and Caribbean Sea atmosphere, *J. Climate*, 24, 893–908, <https://doi.org/10.1175/2010JCLI3496.1>, 2011.
- Dunion, J. P. and Marron, C. S.: A Reexamination of the Jordan Mean Tropical Sounding Based on Awareness of the Saharan Air Layer: Results from 2002, *J. Climate*, 21, 5242–5253, <https://doi.org/10.1175/2008JCLI1868.1>, 2008.
- Dunion, J. P. and Velden, C. S.: The Impact of the Saharan Air Layer on Atlantic Tropical Cyclone Activity, *Bull. Amer. Meteor. Soc.*, 85, 353–366, <https://doi.org/10.1175/BAMS-85-3-353>, 2004.
- Espinosa, A., Miranda, J., and Pineda, J.: Uncertainty evaluation in correlated quantities: application to elemental analysis of atmospheric aerosols, *Rev. Mex. Fis.*, E56, 134–140, 2010.
- Espinosa, A., Reyes-Herrera, J., Miranda, J., Mercado, F., Veytia, M., Cuautle, M., and Cruz, J.: Development of an X-ray fluorescence spectrometer for environmental science applications, *Instrum. Sci. Technol.*, 40, 603–617, <https://doi.org/10.1080/10739149.2012.693560>, 2012.
- Evan, A. T., Dunion, J., Foley, J. A., Heidinger, A. K., and Velden, C. S.: New evidence for a relationship between Atlantic tropical cyclone activity and African dust outbreaks, *Geophys. Res. Lett.*, 33, L19813, <https://doi.org/10.1029/2006GL026408>, 2006.
- Foltz, G. R. and McPhaden, M. J.: Trends in Saharan dust and tropical Atlantic climate during 1980–2006, *Geophys. Res. Lett.*, 35, L20706, <https://doi.org/10.1029/2008GL035042>, 2008.
- Ganor, E. and Mamane, Y.: Transport of Saharan dust across the eastern Mediterranean, *Atmos. Environ.*, 16, 581–587, [https://doi.org/10.1016/0004-6981\(82\)90167-6](https://doi.org/10.1016/0004-6981(82)90167-6), 1982.
- Ganor, E., Osetinsky, I., Stupp, A., and Alpert, P.: Increasing trend of African dust, over 49 years, in the eastern Mediterranean, *J. Geophys. Res.*, 115, D07201, <https://doi.org/10.1029/2009JD012500>, 2010.
- Gelaro, R., McCarty, W., Suárez, M. J., Todling, R., Molod, A., Takacs, L., Randles, C. A., Darmenov, A., Bosilovich, M. G., Reichle, R., Wargan, K., Coy, L., Cullather, R., Draper, C., Akella, S., Buchard, V., Conaty, A., da Silva, A. M., Gu, W., Kim, G.-K., Koster, R., Lucchesi, R., Merkova, D., Nielsen, J. E., Parityka, G., Pawson, S., Putman, W., Rienecker, M., Schubert, S. D., Sienkiewicz, M., and Zhao, B.: The Modern-Era Retrospective Analysis for Research and Applications, Version 2 (MERRA-2), *J. Climate*, 30, 5419–5454, <https://doi.org/10.1175/JCLI-D-16-0758.1>, 2017.
- GMAO: MERRA-2 inst1_2d_int_Nx: 2d, 1-Hourly, Instantaneous, Single-Level, Assimilation, Vertically Integrated Diagnostics V5.12.4, Goddard Earth Sciences Data and Information Services Center (GES DISC), Greenbelt, MD, USA, <https://doi.org/10.5067/G0U6NGQ3BLE0>, 2015a.
- GMAO: MERRA-2 inst3_3d_aer_Nv: 3d, 3-Hourly, Instantaneous, Model-Level, Assimilation, Aerosol Mixing Ratio V5.12.4, Goddard Earth Sciences Data and Information Services Center (GES DISC), Greenbelt, MD, USA, <https://doi.org/10.5067/LTVB4GPCOTK2>, 2015b.
- Goudie, A. and Middleton, N. J.: *Desert Dust in the Global System*, Springer, Berlin, Heidelberg, <https://doi.org/10.1007/3-540-32355-4>, 2006.
- Goudie, A. S.: Desert dust and human health disorders, *Environ. Int.*, 63, 101–113, <https://doi.org/10.1016/j.envint.2013.10.011>, 2014.
- Griffin, D. V., Garrison, V. H., Herman, J. R., and Shinn, E.: African desert dust in the Caribbean atmosphere: Microbiology and public health, *Aerobiologia*, 17, 203–213, <https://doi.org/10.1023/A:1011868218901>, 2001.
- Grogan, D. F. P. and Thorncroft, C. D.: The characteristics of African easterly waves coupled to Saharan mineral dust aerosols, *Q. J. R. Meteorol. Soc.*, 145, 1130–1146, <https://doi.org/10.1002/qj.3483>, 2019.
- Guieu, C., Loÿe-Pilot, M. D., Ridame, C., and Thomas, C.: Chemical characterization of the Saharan dust end-member: Some biogeochemical implications for the western Mediterranean Sea, *J. Geophys. Res.*, 107, ACH 5-1–ACH 5-11, <https://doi.org/10.1029/2001JD000582>, 2002.
- Hankes, I. and Marinaro, A.: The impacts of column water vapour variability on Atlantic basin tropical cyclone activity, *Q. J. R. Meteorol. Soc.*, 142, 3026–3035, <https://doi.org/10.1002/qj.2886>, 2016.
- Holloway, C. E. and Neelin, J. D.: Moisture Vertical Structure, Column Water Vapor, and Tropical Deep Convection, *J. Atmos. Sci.*, 66, 1665–1683, <https://doi.org/10.1175/2008JAS2806.1>, 2009.
- Hoose, C. and Möhler, O.: Heterogeneous ice nucleation on atmospheric aerosols: a review of results from laboratory experiments, *Atmos. Chem. Phys.*, 12, 9817–9854, <https://doi.org/10.5194/acp-12-9817-2012>, 2012.
- IAEA: *Manual for QXAS*, International Atomic Energy Agency, Vienna, 1997.
- INEGI: Instituto Nacional de Estadística y Geografía México, Anuario estadístico de Yucatán 2009 / Instituto Nacional de Estadística y Geografía, Gobierno del Estado de Yucatán, México, 2009.
- INEGI: Principales resultados de la Encuesta intercensal 2015: Estados Unidos Mexicanos, 2015.
- INEGI: Anuario estadístico y geográfico de Yucatán 2017, 1–711, available at: https://www.datatur.sectur.gob.mx/ITxEF_Docs/YUC_ANUARIO_PDF.pdf, 2017.
- Jackson, J. M., Liu, H., Laszlo, I., Kondragunta, S., Remer, L. A., Huang, J., and Huang, H. C.: Suomi-NPP VIIRS aerosol algorithms and data products, *J. Geophys. Res.-Atmos.*, 118, 12673–12689, <https://doi.org/10.1002/2013JD020449>, 2013.
- Kalashnikova, O. V. and Kahn, R. A.: Mineral dust plume evolution over the Atlantic from MISR and MODIS aerosol retrievals, *J. Geophys. Res.*, 113, D24204, <https://doi.org/10.1029/2008JD010083>, 2008.
- Kalnay, E.: *Atmospheric modeling, data assimilation and predictability*, Cambridge University Press, Cambridge, 2003.
- Kanji, Z. A., Ladino, L. A., Wex, H., Boose, Y., Burkert-Kohn, M., Cziczo, D. J., and Krämer, M.: Overview of ice nucleating particles, *Meteorol. Monogr.*, 58, 1.1–1.33, <https://doi.org/10.1175/AMSMONOGRAPHS-D-16-0006.1>, 2017.
- Karanasiou, A., Moreno, N., Moreno, T., Viana, M., de Leeuw, F., and Querol, X.: Health effects from Sahara dust episodes in Eu-

- rope: Literature review and research gaps, *Environ. Int.*, 47, 107–114, <https://doi.org/10.1016/j.envint.2012.06.012>, 2012.
- Karyampudi, V. M. and Carlson, T. N.: Analysis and Numerical Simulations of the Saharan Air Layer and Its Effect on Easterly Wave Disturbances, *J. Atmos. Sci.*, 45, 3102–3136, [https://doi.org/10.1175/1520-0469\(1988\)045<3102:AANSOT>2.0.CO;2](https://doi.org/10.1175/1520-0469(1988)045<3102:AANSOT>2.0.CO;2), 1988.
- Kaufman, Y. J., Koren, I., Remer, L. A., Tanré, D., Ginoux, P., and Fan, S.: Dust transport and deposition observed from the Terra-Moderate Resolution Imaging Spectroradiometer (MODIS) spacecraft over the Atlantic Ocean, *J. Geophys. Res.*, 110, D10S12, <https://doi.org/10.1029/2003JD004436>, 2005.
- Kloster, S., Feichter, J., Maier-Reimer, E., Six, K. D., Stier, P., and Wetzell, P.: DMS cycle in the marine ocean-atmosphere system – a global model study, *Biogeosciences*, 3, 29–51, <https://doi.org/10.5194/bg-3-29-2006>, 2006.
- Koren, I., Kaufman, Y. J., Washington, R., Todd, M. C., Rudich, Y., Martins, J. V., and Rosenfeld, D.: The Bodélé depression: A single spot in the Sahara that provides most of the mineral dust to the Amazon forest, *Environ. Res. Lett.*, 1, 014005, <https://doi.org/10.1088/1748-9326/1/1/014005>, 2006.
- Korte, L. F., Pausch, F., Trimborn, S., Brussaard, C. P. D., Brummer, G.-J. A., van der Does, M., Guerreiro, C. V., Schreuder, L. T., Munday, C. I., and Stuut, J.-B. W.: Effects of dry and wet Saharan dust deposition in the tropical North Atlantic Ocean, *Biogeosciences Discuss.*, <https://doi.org/10.5194/bg-2018-484>, 2018.
- Kramer, S. J., Kirtman, B. P., Zuidema, P., and Ngan, F.: Subseasonal variability of elevated dust concentrations over South Florida, *J. Geophys. Res.-Atmos.*, 125, e2019JD031874, <https://doi.org/10.1029/2019JD031874>, 2020.
- Lenes, J., Prospero, J., Landing, W., Virmani, J., and Walsh, J.: A model of Saharan dust deposition to the eastern Gulf of Mexico, *Mar. Chem.*, 134–135, 1–9, <https://doi.org/10.1016/j.marchem.2012.02.007>, 2012.
- Liu, Z., Omar, A., Vaughan, M., Hair, J., Kittaka, C., Hu, Y., Powell, K., Trepte, C., Winker, D., Hostetler, C., Ferrare, R., and Pierce, R.: CALIPSO lidar observations of the optical properties of Saharan dust: A case study of long-range transport, *J. Geophys. Res.*, 113, D07207, <https://doi.org/10.1029/2007JD008878>, 2008.
- Li-Jones, X. and Prospero, J. M.: Variations in the size distribution of non-sea-salt sulfate aerosol in the marine boundary layer at Barbados: Impact of African dust, *J. Geophys. Res.-Atmos.*, 103, 16073–16084, <https://doi.org/10.1029/98JD00883>, 1998.
- Linke, C., Möhler, O., Veres, A., Mohácsi, Á., Bozóki, Z., Szabó, G., and Schnaiter, M.: Optical properties and mineralogical composition of different Saharan mineral dust samples: a laboratory study, *Atmos. Chem. Phys.*, 6, 3315–3323, <https://doi.org/10.5194/acp-6-3315-2006>, 2006.
- Middleton, N. J. and Goudie, A. S.: Saharan dust: Sources and trajectories, *T. I. Brit. Geogr.*, 26, 165–181, <https://doi.org/10.1111/1475-5661.00013>, 2001.
- Muñoz-Salazar J., Raga, G. B., Yakobi-Hancock, J., Kim, J. S., Rosas, D., Caudillo, L., Alvarez-Ospina, H., and Ladino, L. A.: Ultrafine Aerosol Particles in the Western Caribbean: A first case study in Merida, *Atmos. Pollut. Res.*, 11, 1767–1775, <https://doi.org/10.1016/j.apr.2020.07.008>, 2020.
- Nenes, A., Murray, B., and Bougiatioti, A.: Mineral dust and its microphysical interactions with clouds, in: *Mineral Dust*, 287–325, Springer, Dordrecht, 2014.
- Orellana, R., Espadas, C., Conde, C., and Gay, C.: Atlas. Escenarios de cambio climático en la Península de Yucatán. Centro de Investigación Científica de Yucatán, Centro de Ciencias de la Atmósfera-Universidad Nacional Autónoma de México, Consejo Nacional de Ciencia y Tecnología, Gobierno de Yucatán, Yucatán México, 2009.
- Perez, L., Tobias, A., Querol, X., Künzli, N., Pey, J., Alastuey, A., Viana, M., Valero, N., González-Cabré, M., and Sunyer, J.: Coarse Particles From Saharan Dust and Daily Mortality, *Epidemiology*, 19, 800–807, <https://doi.org/10.1097/EDE.0b013e31818131cf>, 2008.
- Perry, K. D., Cahill, T. A., Eldred, R. A., Dutcher, D. D., and Gill, T. E.: Long-range transport of North African dust to the eastern United States, *J. Geophys. Res.*, 102, 11225–11238, <https://doi.org/10.1029/97JD00260>, 1997.
- Pey, J., Querol, X., Alastuey, A., Forastiere, F., and Stafoggia, M.: African dust outbreaks over the Mediterranean Basin during 2001–2011: PM10 concentrations, phenomenology and trends, and its relation with synoptic and mesoscale meteorology, *Atmos. Chem. Phys.*, 13, 1395–1410, <https://doi.org/10.5194/acp-13-1395-2013>, 2013.
- Plasencia, A. P.: La Península de Yucatán en el Archivo General de la Nación, UNAM, 1998.
- ProAire.: Programa de Gestión para mejorar la calidad del aire del estado de Yucatán, 1–159, 2018.
- Prodi, F. and Fea, G.: A case of transport and deposition of Saharan dust over the Italian Peninsula and southern Europe, *J. Geophys. Res.-Oceans*, 84, 6951–6960, <https://doi.org/10.1029/JC084iC11p06951>, 1979.
- Prospero, J. M. and Carlson, T. N.: Vertical and areal distribution of Saharan dust over the western equatorial north Atlantic Ocean, *J. Geophys. Res.*, 77, 5255–5265, <https://doi.org/10.1029/JC077i027p05255>, 1972.
- Prospero, J. M.: Long-term measurements of the transport of African mineral dust to the southeastern United States: Implications for regional air quality, *J. Geophys. Res.*, 104, 15917–15927, <https://doi.org/10.1029/1999JD900072>, 1999.
- Prospero, J. M. and Lamb, P. J.: African Droughts and Dust Transport to the Caribbean: Climate Change Implications, *Science*, 302, 1024–1027, <https://doi.org/10.1126/science.1089915>, 2003.
- Prospero, J. M. and Mayol-Bracero, O. L.: Understanding the Transport and Impact of African Dust on the Caribbean Basin, *Bull. Am. Meteor. Soc.*, 94, 1329–1337, <https://doi.org/10.1175/BAMS-D-12-00142.1>, 2013.
- Prospero, J. M., Glaccum, R. A., and Nees, R. T.: Atmospheric transport of soil dust from Africa to South America, *Nature*, 289, 570–572, <https://doi.org/10.1038/289570a0>, 1981.
- Prospero, J. M., Olmez, I., and Ames, M.: Al and Fe in PM_{2.5} and PM₁₀ Suspended Particles in South-Central Florida: The Impact of the Long Range Transport of African Mineral Dust, *Water Air Soil Poll.*, 125, 291–317, <https://doi.org/10.1023/A:1005277214288>, 2001.
- Prospero, J. M., Ginoux, P., Torres, O., Nicholson, S. E., and Gill, T. E.: Environmental characterization of global sources of atmospheric soil dust identified with the Nimbus 7 Total Ozone Mapping Spectrometer (TOMS) absorbing aerosol product, *Rev.*

- Geophys., 40, 1–31, <https://doi.org/10.1029/2000RG000095>, 2002.
- Prospero, J. M., Blades, E., Mathison, G., and Naidu, R.: Interhemispheric transport of viable fungi and bacteria from Africa to the Caribbean with soil dust, *Aerobiologia*, 21, 1–19, <https://doi.org/10.1007/s10453-004-5872-7>, 2005.
- Prospero, J. M., Collard, F.-X., Molinié, J., and Jeannot, A.: Characterizing the annual cycle of African dust transport to the Caribbean Basin and South America and its impact on the environment and air quality, *Global Biogeochem. Cy.*, 29, 757–773, <https://doi.org/10.1002/2013GB004802>, 2014.
- Prospero, J. M., Barkley, A. N., Gaston, C. J., Gatineau, A., Campos y Sansano, A., and Panechou, K.: Characterizing and Quantifying African Dust Transport and Deposition to South America: Implications for the Phosphorus Budget in the Amazon Basin, *Global Biogeochem. Cy.*, 34, e2020GB006536, <https://doi.org/10.1029/2020GB006536>, 2020.
- Provençal, S., Buchard, V., da Silva, A. M., Leduc, R., and Barrette, N.: Evaluation of PM surface concentrations simulated by Version 1 of NASA's MERRA Aerosol Reanalysis over Europe, *Atmos. Pollut. Res.*, 8, 374–382, <https://doi.org/10.1016/j.apr.2016.10.009>, 2017.
- Querol, X., Tobías, A., Pérez, N., Karanasiou, A., Amato, F., Stafoggia, M., Pérez García-Pando, C., Ginoux, P., Forastiere, F., Gumy, S., Mudu, P., and Alastuey, A.: Monitoring the impact of desert dust outbreaks for air quality for health studies, *Environ. Int.*, 130, 104867, <https://doi.org/10.1016/j.envint.2019.05.061>, 2019.
- Randles, C. A., da Silva, A. M., Buchard, V., Colarco, P. R., Darmenov, A., Govindaraju, R., Smirnov, A., Holben, B., Ferrare, R., Hair, J., Shinzuka, Y., and Flynn, C. J.: The MERRA-2 Aerosol Reanalysis, 1980 Onward. Part I: System Description and Data Assimilation Evaluation, *J. Climate*, 30, 6823–6850, <https://doi.org/10.1175/jcli-d-16-0609.1>, 2017.
- Reid, J. S., Jonsson, H. H., Maring, H. B., Smirnov, A., Savoie, D. L., Cliff, S. S., Reid, E. A., Livingston, J. M., Meier, M. M., Dubovik, O., and Tsay, S. C.: Comparison of size and morphological measurements of coarse mode dust particles from Africa, *J. Geophys. Res.*, 108, <https://doi.org/10.1029/2002JD002485>, 2003a.
- Reid, E. A., Reid, J. S., Meier, M. M., Dunlap, M. R., Cliff, S. S., Broumas, A., Perry, K., and Maring, H.: Characterization of African dust transported to Puerto Rico by individual particle and size segregated bulk analysis, *J. Geophys. Res.*, 108, 8591, <https://doi.org/10.1029/2002JD002935>, 2003b.
- Resch, F., Sunnu, A., and Afeti, G.: Saharan dust flux and deposition rate near the Gulf of Guinea, *Tellus B*, 60, 98–105, <https://doi.org/10.1111/j.1600-0889.2007.00286.x>, 2008.
- Rienecker, M. M., Suarez, M. J., Gelaro, R., Todling, R., Bacmeister, J., Liu, E., Bosilovich, M. G., Schubert, S. D., Takacs, L., Kim, G.-K., Bloom, S., Chen, J., Collins, D., Conaty, A., da Silva, A., Gu, W., Joiner, J., Koster, R. D., Lucchesi, R., Molod, A., Owens, T., Pawson, S., Pegion, P., Redder, C. R., Reichle, R., Robertson, F. R., Ruddick, A. G., Sienkiewicz, M., and Woollen, J.: NASA's Modern-Era Retrospective Analysis for Research and Applications, *J. Climate*, 24, 3624–3648, <https://doi.org/10.1175/JCLI-D-11-00015.1>, 2011.
- Rodriguez-Gomez, C., Ramirez-Romero, C., Cordoba, F., Raga, G. B., Salinas, E., Martinez, L., Rosas, I., Quintana, E. T., Maldonado, L. A., Rosas, D., Amador, T., Alvarez, H., and Ladino, L. A.: Characterization of culturable airborne microorganisms in the Yucatan Peninsula, *Atmos. Environ.*, 223, 117183, <https://doi.org/10.1016/j.atmosenv.2019.117183>, 2020.
- Rosinski, J., Haagenson, P., Nagamoto, C., Quintana, B., Parungo, F., and Hoyt, S.: Ice-forming nuclei in air masses over the Gulf of Mexico, *J. Aerosol Sci.*, 19, 539–551, [https://doi.org/10.1016/0021-8502\(88\)90206-6](https://doi.org/10.1016/0021-8502(88)90206-6), 1988.
- Ryder, C. L., Highwood, E. J., Walser, A., Seibert, P., Philipp, A., and Weinzierl, B.: Coarse and giant particles are ubiquitous in Saharan dust export regions and are radiatively significant over the Sahara, *Atmos. Chem. Phys.*, 19, 15353–15376, <https://doi.org/10.5194/acp-19-15353-2019>, 2019.
- Salvador, P., Alonso-Pérez, S., Pey, J., Artíñano, B., de Bustos, J. J., Alastuey, A., and Querol, X.: African dust outbreaks over the western Mediterranean Basin: 11-year characterization of atmospheric circulation patterns and dust source areas, *Atmos. Chem. Phys.*, 14, 6759–6775, <https://doi.org/10.5194/acp-14-6759-2014>, 2014.
- Schutgens, N. A. J., Miyoshi, T., Takemura, T., and Nakajima, T.: Applying an ensemble Kalman filter to the assimilation of AERONET observations in a global aerosol transport model, *Atmos. Chem. Phys.*, 10, 2561–2576, <https://doi.org/10.5194/acp-10-2561-2010>, 2010.
- Shao, Y., Wyrwoll, K.-H., Chappell, A., Huang, J., Lin, Z., McTainsh, G. H., Mikami, M., Tanaka, T. Y., Wang, X., and Yoon, S.: Dust cycle: An emerging core theme in Earth system science, *Aeolian Res.*, 2, 181–204, <https://doi.org/10.1016/j.aeolia.2011.02.001>, 2011.
- Stein, A. F., Draxler, R. R., Rolph, G. D., Stunder, B. J. B., Cohen, M. D., and Ngan, F.: NOAA's HYSPLIT Atmospheric Transport and Dispersion Modeling System, *Bull. Am. Meteorol. Soc.*, 96, 2059–2077, <https://doi.org/10.1175/BAMS-D-14-00110.1>, 2015.
- Tegen, I., Werner, M., Harrison, S. P., and Kohfeld, K. E.: Relative importance of climate and land use in determining present and future global soil dust emission, *Geophys. Res. Lett.*, 31, L05105, <https://doi.org/10.1029/2003GL019216>, 2004.
- Thermo Fisher Scientific Inc.: Instruction Manual for Thermo Scientific Model FH62C14 Ambient Particulate Monitor, available at: <https://assets.thermofisher.com/TFS-Assets/null/{%}7Cnull/Package-Inserts/EPM-manual-FH62C14.pdf> (last access: February 2020), 2007.
- Trapp, J. M., Millero, F. J., and Prospero, J. M.: Temporal variability of the elemental composition of African dust measured in trade wind aerosols at Barbados and Miami, *Mar. Chem.*, 120, 71–82, <https://doi.org/10.1016/j.marchem.2008.10.004>, 2010.
- Tsamalis, C., Chédin, A., Pelon, J., and Capelle, V.: The seasonal vertical distribution of the Saharan Air Layer and its modulation by the wind, *Atmos. Chem. Phys.*, 13, 11235–11257, <https://doi.org/10.5194/acp-13-11235-2013>, 2013.
- Vallina, S. M. and Simó, R.: Strong Relationship Between DMS and the Solar Radiation Dose over the Global Surface Ocean, *Science*, 315, 506–508, <https://doi.org/10.1126/science.1133680>, 2007.

- Venero-Fernández, S. J.: Saharan Dust Effects on Human Health: A Challenge for Cuba's Researchers, *MEDICC Rev.*, 18, 32–34, <https://doi.org/10.1590/MEDICC.2016.18300011>, 2016.
- Veselovskii, I., Goloub, P., Podvin, T., Tanre, D., da Silva, A., Colarco, P., Castellanos, P., Korenskiy, M., Hu, Q., Whiteman, D. N., Pérez-Ramírez, D., Augustin, P., Fourmentin, M., and Kolgotin, A.: Characterization of smoke and dust episode over West Africa: comparison of MERRA-2 modeling with multi-wavelength Mie–Raman lidar observations, *Atmos. Meas. Tech.*, 11, 949–969, <https://doi.org/10.5194/amt-11-949-2018>, 2018.
- Voss, K. K. and Evan, A. T.: A New Satellite-Based Global Climatology of Dust Aerosol Optical Depth, *J. Appl. Meteorol. Clim.*, 59, 83–102, <https://doi.org/10.1175/JAMC-D-19-0194.1>, 2020.
- Walker, G. P. L.: Generation and dispersal of fine ash and dust by volcanic eruptions, *J. Volcanol. Geotherm. Res.*, 11, 81–92, [https://doi.org/10.1016/0377-0273\(81\)90077-9](https://doi.org/10.1016/0377-0273(81)90077-9), 1981.
- Weinzierl, B., Ansmann, A., Prospero, J. M., Althausen, D., Benker, N., Chouza, F., Dollner, M., Farrell, D., Fomba, W. K., Freudenthaler, V., Gasteiger, J., Groß, S., Haarig, M., Heinold, B., Kandler, K., Kristensen, T. B., Mayol-Bracero, O. L., Müller, T., Reitebuch, O., Sauer, D., Schäfler, A., Schepanski, K., Spanu, A., Tegen, I., Toledano, C., and Walser, A.: The Saharan Aerosol Long-Range Transport and Aerosol–Cloud-Interaction Experiment: Overview and Selected Highlights. *Bull. Am. Meteor. Soc.*, 98, 1427–1451, <https://doi.org/10.1175/BAMS-D-15-00142.1>, 2016.
- WHO: Office of World Health Reporting, Quantifying Selected Major Risks to Health. In *The world health report 2002: Reducing risks, promoting healthy life*, World Health Organization, available at: <https://apps.who.int/iris/handle/10665/67454> (last access: March 2020), 2018.
- Wilker, E. H., Preis, S. R., Beiser, A. S., Wolf, P. A., Au, R., Kloog, I., Li, W., Schwartz, J., Koutrakis, P., DeCarli, C., Seshadri, S., and Mittleman, M. A.: Long-term exposure to fine particulate matter, residential proximity to major roads and measures of brain structure, *Stroke*, 46, 1161–1166, <https://doi.org/10.1161/STROKEAHA.114.008348>, 2015.
- World Resource Institute.: *Inventario Municipal de Gases de Efecto Invernadero Municipio de Mérida, 1–29*, available at: http://www.merida.gob.mx/municipio/sitiosphp/sustentable/contenidos/doc/Inventario_Municipal_GEI.pdf, (last access: January 2021), 2018.
- Zhang, H., McFarquhar, G. M., Saleeby, S. M., and Cotton, W. R.: Impacts of Saharan dust as CCN on the evolution of an idealized tropical cyclone, *Geophys. Res. Lett.*, 34, L14812, <https://doi.org/10.1029/2007GL029876>, 2007.
- Zhang, J. and Reid, J. S.: MODIS aerosol product analysis for data assimilation: Assessment of over-ocean level 2 aerosol optical thickness retrievals, *J. Geophys. Res.*, 111, D22207, <https://doi.org/10.1029/2005JD006898>, 2006.
- Zhang, X., Zhao, L., Tong, D. Q., Wu, G., Dan, M., and Teng, B.: A systematic review of global desert dust and associated human health effects, *Atmosphere-Basel*, 7, 158, <https://doi.org/10.3390/atmos7120158>, 2016.